In-Situ Gamma-Ray Assay of the 235-F Plutonium Fuel Form Facility at the Savannah River Site – 16293

Alexander Couture *, David DiPrete **, John Musall ***, Donald Pak **, Michael Gilles ***, Timothy Aucott **, Alexander Brand **
* Pajarito Scientific Corporation
** Savannah River National Laboratory
*** Savannah River Nuclear Solutions

ABSTRACT

The Plutonium Fuel Form (PuFF) Facility is located in Building 235-F near the geographic center of the Savannah River Site. Between 1978 and 1984, the facility was used to produce approximately 165 kilograms of iridium-encapsulated Pu-238 spheres and pellets for use as radioisotope thermal generators, primarily for the space program. The facility is divided between two cell lines, the east cell line used to process powdered Pu-238 oxide raw material into fuel forms and the west cell line used to encapsulate the fuel forms in iridium.

Scoping in-situ gamma-ray assays were performed in the PuFF Facility in 2006 and estimated that hundreds of grams of Pu-238 holdup were within the facility. Using this holdup estimate as a source term, SRS has performed a risk analysis that indicated a seismic event that induces a full-facility fire in 235-F could lead to a 28,800 rem dose to a co-located worker. Based on this risk assessment, SRS is taking steps to decontaminate the facility. One of the first steps taken has been to improve upon the quality of the in-situ gamma-ray assay data.

Carts and collimators were specially designed to survey the equipment in the PuFF Facility. The cell interiors were assayed along with the furnaces and storage coolers that protrude beneath the cells. While the previous scoping work consisted of 32 measurements, the current series of measurements included nearly 400 measurements using both high-purity germanium and lanthanum bromide detectors. Data analysis for the current set of measurements was conducted with greater rigor as well. MCNP5 was used to evaluate a variety of possible physical distributions for the Pu-238 source term and estimate cross-talk between neighboring cells. Data analysis was performed using three gamma-rays emitted by Pu-238 (99.85 keV, 152.7 keV, and 766.4 keV) providing three independent estimates of the mass of Pu-238 holdup in each of the cells. This also allowed the application of matrix correction factors to adjust gamma-ray attenuation. The weighted mean of these three results was used as the best estimate of Pu-238 holdup in the PuFF facility. This work lowered the estimate of holdup in the PuFF facility by approximately 100 grams compared to the previous estimate, a 0.55σ difference. The uncertainty in the Pu-238 holdup was also reduced substantially relative to the 2006 scoping assay.

Further radiological measurements are planned for the near future including in-situ gamma-ray assays of wing cabinets in the east cell line maintenance area, the transfer tube between the two cell lines, and some of the furnaces and storage coolers. A germanium gamma imager, the GeGI, will also be used to map out the distribution of the Pu-238 source term in the PuFF Facility.

INTRODUCTION

The Plutonium Fuel Form (PuFF) Facility is located in Building 235-F near the geographic center of the Savannah River Site. The facility was used to produce iridium-encapsulated Pu-238 spheres and pellets for use as radioisotope thermal generators, primarily for the space program. The facility is divided between two cell lines, the East Cell Line (Cells 1-5) used to process the powdered Pu-238 oxide raw material into fuel forms and the West Cell Line (Cells 6-9) used to encapsulate the fuel forms in iridium. Between 1978 and 1984, the PuFF Facility processed approximately 165 kilograms of Pu-238. In 1984, the facility was placed in "enhanced readiness mode", which consisted of reducing staff to the minimum required to keep the facility maintained in operating condition while waiting for a new mission. During this time, the inert argon atmosphere in the east cell line was not maintained. The purpose of the inert argon atmosphere was to prevent corrosion from the high-alpha activity of Pu-238. Corrosion soon made the East Cell Line inoperable, particularly the aluminum remote manipulators. The facility has not been decontaminated since the intent was to continue operations and after the failure of the manipulators much of the facility is inaccessible [1]. Powder processing in the East Cell Line resulted in significant airborne contamination, which coated the interiors of Cells 1-5. In contrast, solid pellets and spheres were handled in the West Cell Line resulting in less airborne contamination and less surface contamination. Based on this process knowledge, holdup in the West Cell Line is expected to be (and was found to be) much less than the holdup in the East Cell Line.

Scoping in-situ gamma-ray assays were performed in the PuFF Facility in 2006 [2]. The current estimate of Pu-238 holdup in the facility is based upon these measurements. Using this holdup estimate as a source term, SRS has performed a risk analysis that indicated a seismic event that induces a full-facility fire in 235-F could lead to a 28,800 rem dose to a co-located worker [3]. Based on this risk assessment, SRS is taking steps to decontaminate the facility. One of the first steps taken has been to improve upon the quality of the in-situ gamma-ray assay data. Carts and collimators were specially designed to survey the equipment in the PuFF Facility. While the previous scoping work consisted of 32 measurements [2], the current series of assay measurements included nearly 400 measurements, with most of this increase occurring on the East Cell Line. Data analysis for the current set of measurements was conducted with greater rigor as well. MCNP5 [4] was used to evaluate a variety of possible physical distributions for the Pu-238 source term and estimate cross-talk between neighboring cells.

DATA COLLECTION

On August 29th, 2013, scientists from SRNL took a series of in-situ gamma-ray measurements in the maintenance trench beneath Cells 6-9 on the West Cell Line of the PuFF facility. Then, on September 17th-19th, 2013, scientists from SRNL took a series of in-situ gamma-ray measurements in the maintenance trench beneath Cells 1-5 on the East Cell Line of the PuFF facility. The detector used was a 20%-efficient, p-type HPGe detector with a 1.27 mm aluminum endcap. The detector's efficiency calibration was verified on the days of the measurements using a Cs-137 check source. A Canberra Lynx MCA was used to provide high-voltage and preamp power to the detector as well as process the detector signals. A Panasonic TOUGHBOOK tablet computer was used to run Canberra's Genie 2000 software [5], which controlled the MCA and saved the spectral data. A specialized cart was fabricated to hold the detector in a vertical orientation, aimed at the floor of the cells above. A second cart was used to hold the detector in a horizontal orientation to assay the furnaces and storage coolers that protruded beneath the cell floors. The detector, LN dewar, signal cables, Lynx MCA, and tablet computer were all wrapped in plastic to prevent Pu-238 contamination. A large tungsten-shot collimator was used for all data acquisitions on the East Cell Line. The tungsten shot collimator was a stainless steel canister that shielded the sides of the detector crystal with 4.2 cm of tungsten shot and the face with 10.16 cm. The hole in the collimator was 4.12 cm in diameter, which narrowed the detector's view of the floor to a roughly 75 cm diameter circular region. A tungsten shot plug was used to occlude the collimator hole for background measurements. Initial data acquisitions were attempted on the West Cell Line using the tungsten-shot collimator. The count rates obtained in this manner were unreasonably low, thus data on the West Cell Line were taken with the detector completely un-collimated.

On the West Cell Line, Seven fifteen-minute measurements were taken, three beneath Cell 6, two beneath Cell 7, and one beneath each of Cells 8 and 9. The major gamma-rays (99.85 keV, 152.7 keV, and 766.4 keV) of Pu-238 were clearly present in all acquired spectra except the spectrum taken under Cell 9. The gamma-ray energies found in the spectrum acquired under Cell 9 are associated with K-40 and the decay chain of Th-232, both naturally occurring radioisotopes. During all measurements, the face of the detector was located 106.7 cm beneath the floor of the cells. The location of the detector in the plane parallel to the cell floor was recorded for each measurement. A diagram showing the approximate location of each measurement in relation to the West Cell Line geometry is shown in Figure 1.

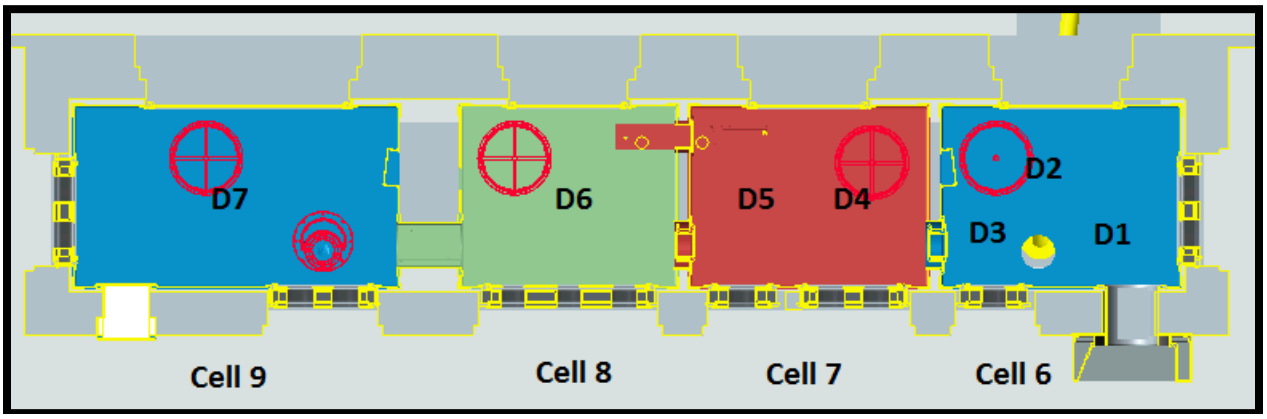

Figure 1: West Cell Line Geometry and Assay Positions. Assay locations are denoted by numbered "D"s.

For the assay of the East Cell Line, all spectral acquisitions were taken with two minutes live time, however the northern furnace in Cell 1 was assayed four times consecutively in the same location. Twenty-nine spectra were taken of the Cell 1 floor, ten of Cell 2, ten of Cell 3, thirteen of Cell 4, and seven of Cell 5. A diagram showing the approximate location of each floor measurement in relation to the East Cell Line geometry is shown in Figure 2. Measurements were taken of all oxygen exchange furnaces and coolers except the Cell 5 cooler, which was inaccessible with the horizontal detector cart. The southern end of Cell 5 was inaccessible to the vertical detector cart because access stairs to the maintenance trench were in the way.

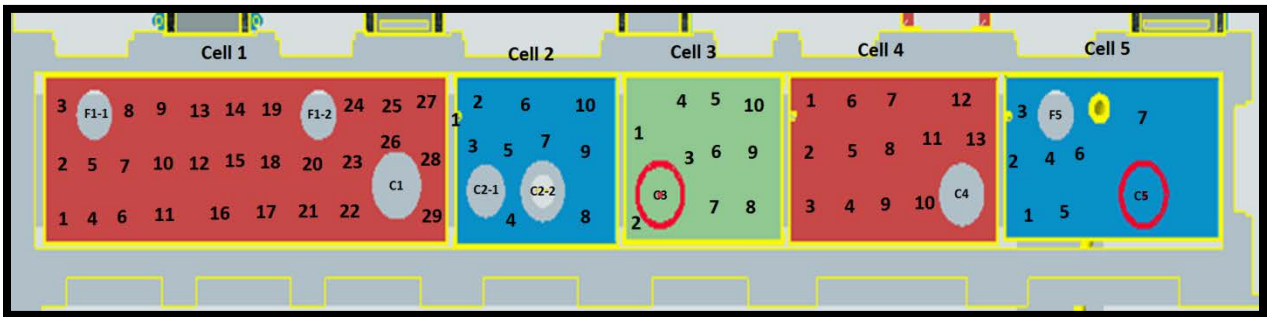

Figure 2: East Cell Line Geometry and Assay Locations. The assay locations for each cell are indicated by numbers. Oxygen-exchange furnaces and coolers are labeled with F or C, respectively, followed by the cell number. If there are multiple furnaces or coolers in the cell, the label is appended with -1 or -2. Cell 1 is on the northern end of the cell line.

Between August 12th and 15th, 2013 a series of scoping measurements were performed on the East Cell Line using a tightly-collimated LaBr detector. Sixty-eight measurements were taken with the detector pointed up at the cell floors viewing of a roughly 40 cm diameter region. Thirty-eight measurements were taken examining the furnaces and coolers that protrude beneath the cell floors. Then on August 28th

and 29th, 2013 another series of scoping measurements were performed on the West Cell Line using the same LaBr detector. Fourteen measurements were taken with the detector pointed up at the cell floors: three in each of Cells 6-8 and 5 in Cell 9. One measurement was taken beneath the cooler in each cell. Twelve measurements were taken with the detector pointed horizontally into the cells flush to the rough center of the Lexan gloveport covers (~38 cm above the cell floors), one in each glove port. During each of these measurements data were acquired for thirty seconds live time. For the most part, these measurements were not used directly in data analysis, but were instead used as supporting evidence for likely distributions of Pu-238 in the East Cell Line. These measurements indicated that the Pu-238 is distributed fairly evenly throughout the cells. The ratio of counts between pairs of Pu-238 gammas in a single spectrum was examined as well. This indicated that the attenuation is relatively uniform as well; there are not locations with significantly more shielding than others.

DATA ANALYSIS

To calculate the mass of Pu-238 in each of the assayed objects the following formula was used:

$$M_{^{238}Pu} = \frac{N_{net}}{S_{^{238}Pu} \cdot BR_{\gamma} \cdot \varepsilon \cdot t} \qquad \text{(Eq. 1)}$$

where,

N_{net} = the net counts in the photopeak (or the minimum detectable counts if applicable),

$S_{^{238}Pu}$ = the specific activity of Pu-238 (6.336×10^{11} Bq/gram ± 0.1%),

BR_{γ} = the absolute branching ratio of the gamma-ray used in the analysis,

t = the assay live time,

and ε = the detector efficiency at the energy of the gamma-ray used for the analysis.

Detector Efficiency

The overall detector efficiency (ε) defined as the probability that a gamma-ray emitted by the Pu-238 is detected by the HPGe detector may be expressed as three independent parameters as follows:

$$\varepsilon = \varepsilon_0 \alpha \, \Omega \qquad \text{(Eq. 2)}$$

where, ε_0 is the energy-dependent intrinsic detector efficiency (the probability that a photon that hits the detector is counted in the photopeak), α is the energy-dependent attenuation coefficient (the fraction of photons emitted in the direction of the detector that arrive unscattered), and Ω is the average solid angle of the detector relative to the source distribution (the fraction of photons emitted by the source emitted in the direction of the detector).The intrinsic detector efficiency is the same for the point source calibration and the detector measurements, excluding effects from the angle of incidence and collimation effects that are taken into account as sources of uncertainty. MCNP calculations were used to estimate the product of the attenuation coefficient and the solid angle, which will be defined as ϕ_{MCNP}, the photon flux (cm^{-2}) at the detector face normalized per source photon (at the energy used for the analysis) from the source distributions modeled. This same parameter may be defined for the point source calibration configuration as ϕ_p, the photon flux (cm^{-2}) at the detector face normalized per source photon from a point source located 38.1 cm from the face of the detector. Thus the detector efficiency for the assay geometry is given as follows:

$$\varepsilon = \varepsilon_p \left(\frac{\phi_{MCNP}}{\phi_p} \right) \qquad \text{(Eq. 3)}$$

where, ε_p is the absolute point source detector efficiency. Making this substitution into Eq. 1, the equation used to calculate the holdup mass of Pu-238 in the cells becomes:

$$M_{^{238}Pu} = \frac{N_{net} \cdot \phi_p}{S_{^{238}Pu} \cdot BR_\gamma \cdot \varepsilon_p \cdot \phi_{MCNP} \cdot t} \qquad \text{(Eq. 4)}$$

Since attenuation is negligible for the point source calibration geometry, the parameter, ϕ_p, and its uncertainty may be calculated as follows:

$$\phi_p = \frac{1}{4\pi r^2} \quad \text{(Eq. 5)}$$

$$\partial\phi_p = \frac{\partial r}{2\pi r^3} \quad \text{(Eq. 6)}$$

Inserting r = 38.1 ± 0.5 cm into Equations 4.5 and 4.6, ϕ_p = 5.48 × 10^{-5} cm^{-2} ± 2.6%.

The uncollimated detector efficiency for the HPGe was measured using two point sources: a Ho-166m source (IPL-1278-38) and a mixture of Eu-152, Eu-154, and Eu-155 (EZ-1480-93-10 and EZ-1480-93-9). The europium isotope blend was produced at SRNL from two liquid standards that were mixed and dried on a planchet. The sources were located 38.1 cm from the face of the detector directly on its central axis. The efficiency curve for this detector was determined using Canberra's Genie 2000 software [5] and is shown in Figure 3. Energy-dependent empirical corrections were made to the collimated measurements to account for occlusion of part of the detector face by the collimator. Additional uncertainty was included in the un-collimated assays to account for variation in detector efficiency at high angles of incidence.

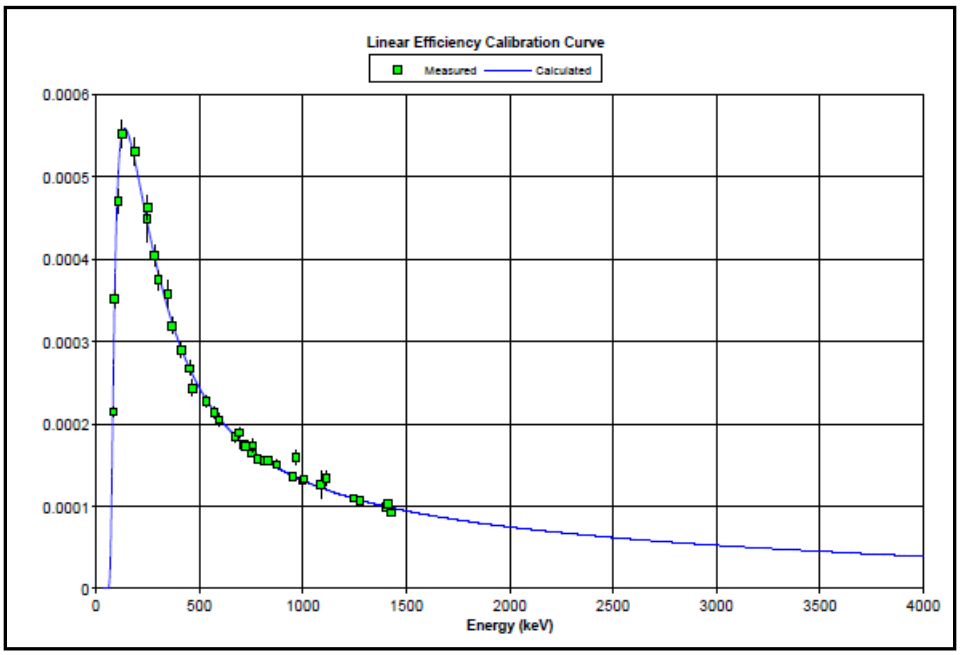

Figure 3: Point Source Efficiency for HPGe Detector located 38.1 cm from Ho-166m, Eu-152, Eu-154, and Eu-155 gamma-ray sources.

MCNP Calculations

To estimate the gamma-ray flux at the detector locations per gamma-ray emitted by Pu-238, a simulation of the east cell line of PuFF was created using the MCNP5 [2] software. This program was used to determine the geometric solid angle of the detector relative to the source geometry as well as correct for attenuation of the gamma-ray flux through intervening material in the cells. A variety of source distributions were modeled to determine the uncertainty associated with the Pu-238 holdup distribution.

The cell interiors particularly on the East Cell Line are not visible because of the lack of interior lighting and the opacity of the cell windows. As such the current contents and distribution of items contained in the cells is uncertain. An inventory of items for each cell was compiled based upon historical drawings, photographs, and process knowledge. Lower, middle, and upper level estimates for the net mass of the cell inventories were developed. These items were approximated as a layer of uniform density, referred to as a "Material Layer" henceforth, distributed in the bottom 30 cm of the cell volumes.

The following source distributions were modeled for the cell interiors:

Floor: Photon source uniformly distributed on the floor of the cells,
Uniform: Photon source uniformly distributed throughout the volume of each cell above the middle-density material representing an airborne distribution,

Material Layer: Photon source uniformly distributed throughout the middle-density material layer,
High Material Layer: Photon source uniformly distributed throughout the high-density material layer,
Low Material Layer (LML): Photon source uniformly distributed throughout the low-density material layer,
Ceiling Material Layer (CML): Photon source uniformly distributed on the ceiling of the cells with the middle-density material layer acting as an attenuator,
Wall Material Layer (WML): Photon source uniformly distributed on the walls of the cells with the middle-density material layer acting as an attenuator,
and **HEPA:** Photon source uniformly distributed within the HEPA filter in each cell with the middle-density material layer acting as an attenuator.

All of the source distribution were not included in the final analysis, for example, the HEPA distribution was not included in the collimated measurements because only certain measurement contained the HEPAs in their field of view and the count rates from those measurements did not differ significantly from their neighbors. The middle-density material layer was used as the best estimate of the assay geometry. Other distributions were used to evaluate total measurement uncertainty and bounding cases. Similar treatment was given to the furnace and storage cooler assay measurements.

Net Counts

The three major gamma-rays emitted by Pu-238 were used for the analysis: 99.85 keV, 152.7 keV, and 766.4 keV. PeakEasy 4.51 [6] software developed by LANL was used to fit and integrate the three photopeaks in each measured spectrum. MDAs were calculated using the standard Currie formula [7]:

$$MDA = 2.71 + 4.65\sqrt{\sigma_{GROSS}^2 + \sigma_{BKG}^2} \qquad \text{(Eq. 5)}$$

Multiple measurements were made of the cell interiors for all cells except for Cells 8 and 9. These series of measurements were treated in the analysis as a single detector array rather than a sequence of independent measurements. For example, the photopeak integrals for the 29 measurement taken under Cell 1 were summed. Likewise, the flux calculated by MCNP for these 29 measurement positions were summed as well.

The measurements beneath the West Cell Line were taken with the detector completely un-collimated. As such, the measurement suffered from considerable cross-talk between neighboring cells. A novel approach was used to correct for this effect using MCNP simulations to estimate the flux on the detectors beneath one cell per source photon arising in another. The simulations were used with the analytical treatment described below.

Consider two cells (or more generally items being assayed), Cell *i* and Cell *j*. If Cell *j* has a substantially greater count rate than Cell *i*, then the following equation is valid:

$$C_{ii} = C_i - \frac{\phi_{ij}}{\phi_{jj}} C_j \qquad \text{(Eq. 6)}$$

where,

C_i = the total number of counts measured beneath Cell *i*,

C_{ij} = the total number of counts measured beneath Cell *i* from photons arising in Cell *j*,

and ϕ_{ij} = the flux on the detectors beneath Cell *i* per photon arising in Cell *j*.

However, if there are substantial counts in Cell *i* from Cell *j* and vice versa, the following equations must be used:

$$C_{ii} = C_i - \frac{\phi_{ij}}{\phi_{jj}} C_{jj} \text{ and } C_{jj} = C_j - \frac{\phi_{ji}}{\phi_{ii}} C_{ii}. \qquad \text{(Eqs. 7 and 8)}$$

This pair of coupled equations may be expanded into an infinite series as follows:

$$C_{ii} = \left(C_i - \frac{\phi_{ij}}{\phi_{jj}} C_j \right) \left[1 + \frac{\phi_{ij}\phi_{ji}}{\phi_{ii}\phi_{jj}} - \left(\frac{\phi_{ij}\phi_{ji}}{\phi_{ii}\phi_{jj}} \right)^2 + \left(\frac{\phi_{ij}\phi_{ji}}{\phi_{ii}\phi_{jj}} \right)^3 - \ldots \right]. \qquad \text{(Eq. 9)}$$

The uncertainty in C_{ii} is given below (neglecting the covariance associated with the ϕ_{ij} terms). For simplicity, the expansion term will be defined as:

$$E_\phi \equiv \left[1 + \frac{\phi_{ij}\phi_{ji}}{\phi_{ii}\phi_{jj}} - \left(\frac{\phi_{ij}\phi_{ji}}{\phi_{ii}\phi_{jj}} \right)^2 + \left(\frac{\phi_{ij}\phi_{ji}}{\phi_{ii}\phi_{jj}} \right)^3 - \ldots \right] \qquad \text{(Eq. 10)}$$

It is sufficient to calculate the uncertainty in the expansion to first order, thus:

$$\partial E_\phi = \left(\frac{\phi_{ij}\phi_{ji}}{\phi_{ii}\phi_{jj}} \right) \sqrt{ \left(\frac{\partial \phi_{ij}}{\phi_{ij}} \right)^2 + \left(\frac{\partial \phi_{ji}}{\phi_{ji}} \right)^2 + \left(\frac{\partial \phi_{ii}}{\phi_{ii}} \right)^2 + \left(\frac{\partial \phi_{jj}}{\phi_{jj}} \right)^2 } \qquad \text{(Eq. 11)}$$

and

$$\partial C_{ii} = \sqrt{E_{\phi}^{2}\left[\partial C_{i}^{2} + \left(\frac{\phi_{ij}}{\phi_{jj}}C_{j}\right)^{2}\left[\left(\frac{\partial\phi_{ij}}{\phi_{ij}}\right)^{2} + \left(\frac{\partial\phi_{jj}}{\phi_{jj}}\right)^{2} + \left(\frac{\partial C_{j}}{C_{j}}\right)^{2}\right]\right] + \partial E_{\phi}^{2}\left(C_{i} - \frac{\phi_{ij}}{\phi_{jj}}C_{j}\right)^{2}} \quad \text{(Eq. 12)}$$

Since the assay measurements taken on the East Cell Line were highly collimated, cross-talk was only a minor effect. Therefore, it was treated as a source of uncertainty rather than being corrected in the assay mass. The relative uncertainty induced by cross talk was estimated using the following equation:

$$\sigma_{CT} = \sum_{i} \frac{M_{i}\varepsilon_{i}^{CT}}{M\varepsilon} \quad \text{(Eq. 13)}$$

where, the summation runs over neighboring cells or other sources of cross talk. The numerator is proportional to the cross talk count rate and the denominator to the count rate from the mass distribution being assayed.

Total Measurement Uncertainty

The components of total measurement uncertainty considered during data analysis were as follows with values given at the 1σ level:

Counting Statistics – The uncertainty associated with counting statistics varied depending on the number of measurements made of a particular item, the count time, the source intensity, and the branching ratio of the gamma-ray used in the analysis. These varied between 0.1% and 30% for the various items measured. For the West Cell Line, cross talk uncertainty was folded in with the counting uncertainty inducing the 30% uncertainty mentioned above.

MCNP Simulation Statistics – MCNP simulations were run until statistics were negligible in most cases. The worst statistics were associated with the 99.85 keV gamma-ray in the furnaces, which were highly attenuating with a statistical uncertainty of 2%.

Cross Talk – Cross talk uncertainty was highly influenced by the source intensity of the item being measured relative to its neighboring items and to a lesser extent the gamma-ray energy ranging from completely negligible to approximately 35%.

Specific Activity – The specific activity of Pu-238 is known to 0.1%.

Branching Ratio – The branching ratios of the Pu-238 gamma-rays are known to the following precision: the 99.85 keV gamma-ray to 1.1%, the 152.7 keV gamma-ray to 0.8% and the 766.4 keV gamma-ray to 9%.

Detector Efficiency Calibration – The uncertainty associated with the point-source detector efficiency calibration was calculated based on point source activity and branching ratios, detector standoff, curve fitting, collimation effects, and angle of incidence. These values ranged from approximately 4% to 20%. The largest effect arose from angle of incidence for the un-collimated 99.85 keV measurements.

Source Distribution and Matrix Attenuation – The uncertainty associated with the combination of Pu-238 distribution within the assayed item was estimated using MCNP simulations and further refined by differential peak analysis. The West Cell Line contained minimal quantities of material (2-3 grams of Pu-238) and thus was assayed with fewer measurements and less analytical rigor than the East Cell Line. Source distribution and matrix attenuation uncertainties ranged from 40% to 70% for the analysis of specific gamma-ray energies. The cell interiors on the East Cell Line contained the bulk of the Pu-238 holdup. Multiply highly collimated measurement across the cell interiors indicated relatively uniform holdup distribution within an individual cell. This allowed analytical treatment of the cell interior assays as a planar source distribution relative to a planar detector array, minimizing source distribution uncertainty. Differential peak analysis further refined the assay results by making small adjustments to the matrix attenuation to bring the assay results from the three major gamma-rays into agreement. The dominant attenuator in the cell interiors was steel. Varying the thickness of the steel attenuator by 1-5 mm in the various MCNP models brought the assay results for the three gamma energies into agreement on the 5-15% level. Similar treatments were applied to the furnaces and storage coolers in the East Cell Line. However, as these items were each assayed from a single location and were highly attenuating with less available information about the source distribution, the associated uncertainties were considerably higher, on the order of 50-70%.

RESULTS AND FUTURE PLANS

The assay results for each of the three energies considered are essentially completely independent measurements (excluding the attenuation correction procedure). The final assay result for the cell interiors and the Cell 1 furnaces were based on the weighted mean of the result for each of the three energies, where the weighting factor is based on the uncertainty of the measurements. Thus the final assay mass and uncertainty are given by the following expressions:

$$\bar{M} = \frac{\sum_{i=1}^{3} \frac{M_{E_i}}{\partial M_{E_i}^2}}{\sum_{i=1}^{3} \frac{1}{\partial M_{E_i}^2}} \quad \text{and} \quad \partial \bar{M} = \left(\sum_{i=1}^{3} \frac{1}{\partial M_{E_i}^2} \right)^{-\frac{1}{2}}. \qquad \text{(Eqs 14 + 15)}$$

When analysis of all three gamma-ray energies resulted in MDAs, the lowest MDA for the three energies analyzed was reported. The final assay masses for the current

assay are reported in Table 1 along with the previous results from the 2006 scoping assay [2]. The cooler in Cell 5 was not assayed with the HPGe detector,

	Current Assay Mass (g)	2006 Scoping Assay Mass (g) [2]
Cell 1 Interior	114 ± 6 (5%)	264.3 ± 166.5 (63%)
Cell 1 North Furnace	17 ± 5 (31%)	N/A
Cell 1 South Furnace	43 ± 13 (28%)	N/A
Cell 1 Cooler	10.7 (MDA)	N/A
Cell 2 Interior	36 ± 3 (9%)	59.7 ± 43.6 (73%)
Cell 2 North Cooler	11.9 ± 1.3 (11%)	N/A
Cell 2 South Cooler	12.7 (MDA)	N/A
Cell 3 Interior	2.5 ± 0.4 (16%)	2.17 ± 1.45 (67%)
Cell 3 Cooler	7.3 (MDA)	N/A
Cell 4 Interior	9.6 ± 0.6 (7%)	9.82 ± 7.27 (74%)
Cell 4 Cooler	22.4 (MDA)	N/A
Cell 5 Interior	8.7 ± 0.5 (6%)	4.58 ± 3.25 (71%)
Cell 5 Cooler	22.9 (MDA)	N/A
Cell 5 Furnace	12.4 (MDA)	N/A
Cell 6 Interior	2.2 ± 0.7 (32%)	1.78 ± 1.21 (68%)
Cell 7 Interior	0.25 ± 0.08 (30%)	0.055 ± 0.045 (82%)
Cell 8 Interior	0.004 (MDA)	0.00784 (MDA)
Cell 9 Interior	0.004 (MDA)	0.00911 (MDA)
Total	240 ± 40 (17%)	340 ± 170 (50%)

Table 1: Current Assay Results compared with 2006 Scoping Measurements [2]. All results refer only to the mass of Pu-238.

because of geometric constraints. The MDAs reported for this cooler are based on the LaBr scoping measurements. Summing the assay results and treating MDAs as, the total holdup in PuFF was 240 ± 40 grams of Pu-238. These results are as expected based upon process knowledge with the vast majority of the holdup located in Cells 1 and 2 in the East Cell Line where fine powder plutonium oxide was size reduced and handled. The total Pu-238 mass determined by the current assay is 100 grams or 0.55σ lower than the 2006 scoping assay results though the previous results did not account for holdup in the furnaces or coolers. These assay results do not include the wing-cabinets in the East Maintenance area or the transfer line between the East and West Cell Lines. Measurements of these areas are planned to be completed in 2016. The accuracy of the assay results may be improved further with additional knowledge of the source distribution. The thick lead glass, water-filled shield windows are in the process of being removed and the cell interiors are to be illuminated in the near future. This will allow additional assay measurements to be performed from the uncontaminated control room. Pixelated, high-purity germanium gamma-ray imaging technology is to be deployed in the near term future to assess the Pu-238 holdup distribution, further refining the quality of the assay data.

REFERENCES

1. “Report of an Investigation into the Deterioration of the Plutonium Fuel Forms Fabrication Facility (PuFF) at the DOE Savannah River Site” Department of Energy – Nuclear Safety, DOE/NS-0002P, (1991).

2. D.W. Roberts. “FAMS Hold-Up Measurements for PuFF Process Cells” Savannah River Site. N-CLC-F-00796, (2006).

3. “Basis for Interim Operation for Building 235-F.” Savannah River Site, U-BIO-F-00003 Revision 1, (2014).

4. X-5 Monte-Carlo Team. “MCNP – A General N-Particle Transport Code, Version 5, Volume 1: Overview and Theory” Los Alamos National Laboratory. LA-UR-03-1987. (2003).

5. “Genie 2000 Spectroscopy Software: Operations Manual.” Canberra Industries, Inc. (2012).

6. B. Rooney, S. Garner, and P. Felsher. PeakEasy 4.51. Los Alamos National Laboratory. LA-CC-13-040, (2013).

7. L.A. Currie. “Limits for Qualitative Detection and Quantitative Determination: Application to Radiochemistry.” Anal. Chem. 40, 586-593 (1968).

8. A.H. Couture and D.P Diprete. “In-Situ Gamma-Ray Assay of the West Cell Line in the 235-F Plutonium Fuel Form Facility.” Savannah River National Laboratory. SRNL-STI-2014-00440, (2014).

9. A.H. Couture and D.P Diprete. “In-Situ Gamma-Ray Assay of the East Cell Line in the 235-F Plutonium Fuel Form Facility.” Savannah River National Laboratory. SRNL-STI-2014-00629, (2014).